Controlled Fast Vacuum Breaking of an AC Short-Circuit Current in a Short-arcing Time

Xiaofei Yao, *Member, IEEE*, Chen Guan, Jian'gang Ding, Shaogui Ai, Kui Ma, Jianhua Wang, *Senior Member, IEEE*, Yingsan Geng, *Senior Member, IEEE*, and Zhiyuan Liu, *Senior Member, IEEE*

***Abstract*—A quick elimination of short-circuit faults in a short time can significantly promote the transient stability of an AC power grid. This paper proposes controlled fast vacuum breaking (CFVB) of a short-circuit current within a short-arcing time. The CFVB technology performs the following: determining a lower-limit opening speed of 3.5 m/s for a 40.5 kV fast vacuum circuit breaker (FVCB), quickly predicting the fault current-zero within 4.0 $\pm$ 0.4 ms to command the FVCB to open at a selected current phase-angle, and optimizing an electromagnetic repulsion actuator with an opening time of 2.5 $\pm$ 0.05 ms to achieve an accurate opening operation. The CFVB technology was deployed in a prototype of single-phase multiple-break 363 kV FVCB to validate its feasibility. The validation involved test duties of T100s(b) and T100a following standards IEC 62271-100 2017 and GB/T 1984–2014. Test results demonstrated that by adopting the CFVB technology, the 363 kV FVCB can successfully interrupt a fault current of 80 kA rms within the first half-wave fault current with a short-arcing time of 2.5 ms. Further application of the CFVB technology could help promote the transient stability of power distribution and transmission systems.**

***Index Terms*—Arcing time, controlled fast vacuum breaking, electromagnetic repulsion actuator, fast vacuum circuit breaker.**

I. Introduction

CONTINUAL growth in generation and consumption of electrical energy and enhanced connectivity of power networks has led to a significant increase in fault currents. Considerable effort has been devoted to technologies that limit or break short-circuit current in various ways to promote the transient stability of a power grid [1], [2]. Current-limiting technologies in such applications as superconductivity, liquid metals, and solid-state permits the power equipment to remain in service even though the prospective short-circuit current exceeds its rated peak and short-time withstand current [3]–[6]. However, it is heavy-duty for a circuit breaker (CB) to directly interrupt a fault current over its rated values, let alone to quickly eliminate the fault in an extremely short time. This is because the opening time of the CB driven by traditional operating mechanisms like those involving springs, permanent magnets, or hydraulics exceeds about 30 ms [7], [8].

There has been renewed interest recently in controlled switching technologies as an introduction of the electromagnetic repulsion actuator (ERA) into developing fast vacuum circuit breakers (FVCBs) [9], [10]. The closing and opening times of the FVCB could be dramatically decreased to several milliseconds and their deviations to tens of microseconds. Moreover, a higher short-circuit breaking current than the rated value of the FVCB can also be achieved in a short-arcing time current interruption as reported in [10]. This is due to the lower arcing energy deposited onto both contact surfaces in the case that a high opening speed is applied to interrupt a high current. Therefore, it is conceivable to use the FVCB to eliminate an over short-circuit fault [10] or limit the exceeding short-circuit current particularly by a superconducting fault current limiter (SFCL) [6], [11] in the first half-wave fault current in conjunction with a system that could quickly identify a short-circuit fault. This could significantly improve the transient stability of the power grid and render a considerable cost saving for an under-planning power network by allowing the application of equipment with lower ratings.

However, there are no such technologies, from the state of the art, that could quickly eliminate a short-circuit fault within a short time for the AC power grid. This paper proposes controlled fast vacuum breaking (CFVB) of a short-circuit current within a short-arcing time. The CFVB technology operates in the following sequence: 1) determining a lower-limit opening speed for the FVCB, 2) quickly predicting a short-circuit current-zero, and 3) optimizing the ERA with a low deviation of opening time.

II. CFVB Technology

A. Lower-Limit Opening Speed for the FVCBs

An opening speed of a vacuum circuit breaker (VCB) has a significant influence on transferring of the vacuum arc anode-discharging modes, which tends to result in a successful current

Manuscript received February 12, 2021; revised April 29, 2021 and May 18, 2021; accepted May 24, 2021. Date of publication June 21, 2021; date of current version July 13, 2021. This work was supported in part by the Key Research and Development Program of Shaanxi Province under Project 2019ZDLGY18-04, and in part by the State Grid Project under Contract 5500-201935401A-0-0-00. *(Corresponding author: Xiaofei Yao.)*

Xiaofei Yao, Chen Guan, Jian'gang Ding, Jianhua Wang, Yingsan Geng, and Zhiyuan Liu are with the State Key Laboratory of Electrical Insulation and Power Equipment, Xi'an Jiaotong University, Xi'an, Shaanxi 710049, China (e-mail: yaoxf85@mail.xjtu.edu.cn; 641497899@qq.com; lbddjg@163.com; jhwang@mail.xjtu.edu.cn; ysgeng@mail.xjtu.edu.cn; liuzy@mail.xjtu.edu.cn).

Shaogui Ai and Kui Ma are with the State Key Laboratory of Electrical Insulation and Power Equipment, Xi'an Jiaotong University, Xi'an, Shaanxi 710049, China and also with the State Grid Ningxia Electric Power Research Institute Company, Ltd., Ningxia 750001, China (e-mail: aishaogui@sina.com; 12976118@qq.com).

Color versions of one or more figures in this article are available at https://doi.org/10.1109/TASC.2021.3091047.

Digital Object Identifier 10.1109/TASC.2021.3091047

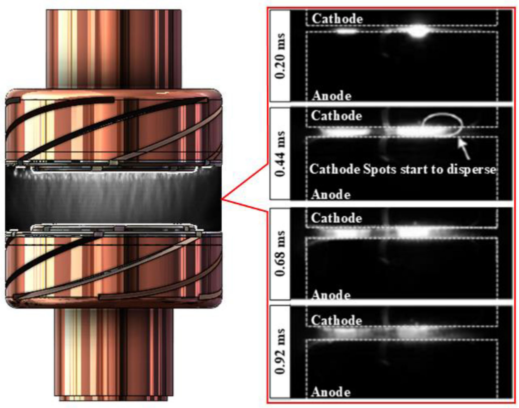

Fig. 1. Geometry of cup-type AMF contacts, and typical evolvement of anode-discharging modes in 40 kA rms current interruption. The total arcing time is 2.0 ms. The intense-arc mode transfers into diffuse-arc mode at an instantaneous arcing time of 0.44 ms.

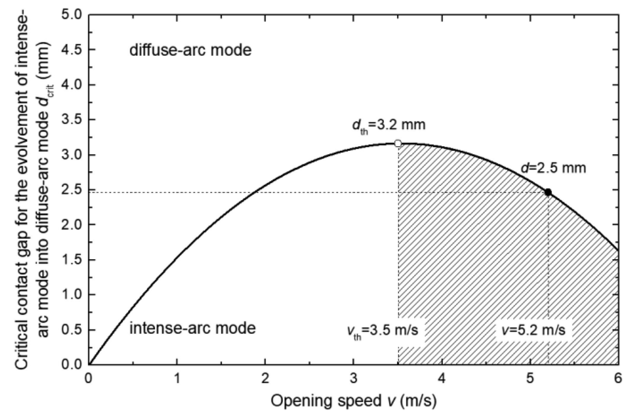

Fig. 2. Dependence of d_{crit} on v for arcing current of 40 kA rms, where v_{th} is a lower-limit opening speed for the 40.5 kV FVCB.

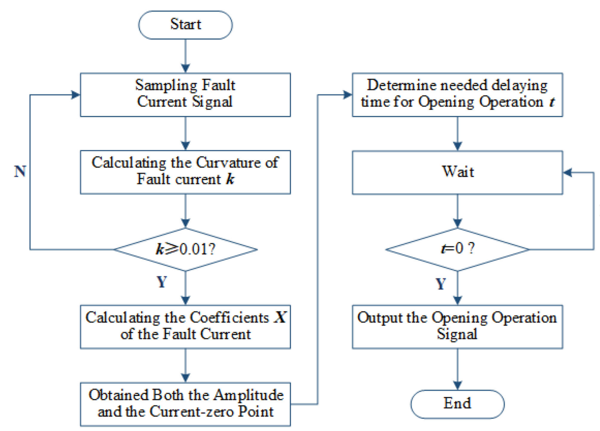

Fig. 3. Flow chart of the quick prediction of fault current-zero program and operating sequence for the CFVB technology.

interruption in a case of long-lasting durations for the diffuse-arc mode [12]. It is essential to acquire an adequate opening speed for the designed FVCB to perform a reliable current interruption within a short-arcing time. Take the commonly used cup-type axial magnetic field (AMF) contacts in VCBs as an example. The evolvement of anode-discharging mode was experimentally investigated for different arcing currents and opening speed. Fig. 1 shows the geometry of cup-type AMF contacts for a 40.5 kV FVCB, together with the observed evolvement of anode-discharging modes in 40 kA rms current interruption.

The evolvement of initial intense-arc mode into diffuse-arc in current interruption was characterized by dispersing motion of multiple cathode spots on cathode surface. The intense-arc only transferred into the diffuse-arc, rather than the footpoint or anode-spot, for various values of arcing current I_{rms} and opening speed v in the first half-wave arcing current. The dependence of the instantaneous arcing time t_{crit} at the mode-evolving point on v and I_{rms} can be statistically obtained as

$$t_{\text{crit}} = -0.253 \cdot v + 0.024 \cdot I_{\text{rms}} + 0.830 \quad (1)$$

where t_{crit} is the critical arcing time for the mode evolvement in ms, v is the opening speed of the FVCB in m/s, and I_{rms} is the rms arcing current in kA.

In this way, the critical contact-gap d_{crit} for the evolvement of intense-arc into diffuse-arc can be obtained by multiplying t_{crit} with v. Fig. 2 shows the dependence of d_{crit} on v for a 40 kA rms current interruption. In fig. 2, the anode-discharging mode would remain in intense-arc in the case that the instantaneous contact-gap d is lower than d_{crit}. Inversely, the intense-arc would quickly evolve into diffuse-arc, which assists a successful current interruption.

Notably, there exists a maximum critical contact-gap d_{th} of 3.2 mm and a corresponding threshold speed v_{th} of 3.5 m/s. The v_{th} is the lower-limit opening speed for the 40.5 kV FVCB. When v is designed to be 5.2 m/s, higher than v_{th}, d_{crit} and t_{crit} decrease from 3.2 to 2.47 mm and from 0.90 to 0.47 ms, respectively. The decreased t_{crit} means a short-lasting duration for the intense-arc mode. Thus, a moderate contact surface erosion, caused by the intense-arc mode, could be achieved.

A series of successful current interruption tests on the 40.5 kV FVCB showed a minimum arcing time of 0.5 ms and a maximum arcing time of 7.8 ms for $v = 5.2$ m/s. Therefore, the higher the designed v is than v_{th} of 3.5 m/s, and the lower the arcing time is than its maximum while remaining higher than its minimum, the better the FVCB successfully interrupts a short-circuit current. Besides, an extended electrical endurance of the FVCB would benefit from a low arcing time in series of high current interruptions.

B. Quick Prediction of Fault Current-Zero

A quick prediction of short-circuit current-zero is necessary to command the FVCB to open at an adequate current phase-angle to complete a successful current interruption. Fig. 3 shows the flow chart of the program for predicting the short-circuit current-zero and the operating sequence for the CFVB technology. Once a short-circuit fault is detected, the program is launched to predict the fault-current-zero and inform the FVCB to open after a time delay t. The time delay t strongly depends on the intrinsic arcing time window (i.e., the time interval between the minimum arcing time and the maximum arcing time) and the opening time of the FVCB.

A fault-identifying algorithm works with the program to predict the current-zero. The algorithm is based on the detection of curvature mutation of current waveform:

$$\Delta\alpha = atan\left(\frac{i_{n+1} - i_n}{T_S}\right) - atan\left(\frac{i_n - i_{n-1}}{T_S}\right) \quad (2)$$

$$\Delta s = \frac{\sqrt{(i_{n+1} - i_n)^2 - T_S^2} - \sqrt{(i_{n+1} - i_n)^2 - T_S^2}}{2} \quad (3)$$

where $\Delta\alpha$ is the angular variation of the current waveform tangent lines between two adjacent sampling points in rad/s; i_{n+1}, i_n, and i_{n-1} are three adjacent current sampling points in kA; Δs is the length between two adjacent points in kA; and T_S is the sampling period in s. In this case, the curvature of current-wave can be obtained as

$$k = \frac{\Delta s}{\Delta\alpha} \cdot T_S \quad (4)$$

where k is the curvature of current-wave in kA·s/rad. Once the absolute value of k rises exceeding a critical value, typically 0.01 in this study, the current is identified as a short-circuit current. The fault-initiated phase-angle could also be available when $k \geq 0.01$ kA·s/rad.

The fault current-zero prediction algorithm is based on the least-squares method. Take the unidirectional short-circuit current I_{SC} as an example, the equation of I_{SC} is

$$\begin{aligned} i_{SC} &= I_m \sin(\omega t + \alpha - \varphi) \\ &\quad + \left[I_{m|0|} \sin\left(\alpha - \varphi_{|0|}\right) - I_m \sin(\alpha - \varphi)\right] e^{-t/\tau} \end{aligned} \quad (5)$$

The parameters of i_{SC} in (5) can be obtained by solving its orthogonal equation

$$i_{SC} = X_1 \sin(\omega t) + X_2 \cos(\omega t) + X_3 \cdot t - X_4 \quad (6)$$

where $X_1 - X_4$ are the coefficients of the fault current equation, which can be resolved by introducing an identity matrix $\mathbf{U}$ and an orthogonal $n \times 4$ matrix $\mathbf{A}$, respectively. The dimension value n for both $\mathbf{U}$ and $\mathbf{A}$ is closely correlated with the sampling rate of the fault current. In this case, the coefficients in (5) are the solutions of (7):

$$\begin{bmatrix} X_1 \\ X_1 \\ X_3 \\ X_4 \end{bmatrix} = \left(\mathbf{A}^T\mathbf{U}^T\mathbf{U}\mathbf{A}\right)^{-1} \cdot \left(\mathbf{A}^T\mathbf{U}^T\mathbf{U}\mathbf{A}\right) \cdot \begin{bmatrix} i_{SC}(t_1) \\ i_{SC}(t_2) \\ \cdots \\ i_{SC}(t_n) \end{bmatrix} \quad (7)$$

where $\mathbf{A}$ is an orthogonal matrix of (6) with dimensions $n \times 4$, $\mathbf{U}$ is an identity matrix with dimensions $n \times n$, and $i_{SC}(t_1) - i_{SC}(t_n)$ are the sampling points of the fault current.

The current-zero prediction program was implemented with an STM32H7B0 microprocessor, a sampling rate of 50 kHz, and a sampling window of 4.0 ms. The sampling window kept sliding in steps of 1.0 ms. In the sliding process, the microprocessor worked to calculate the curvature of the sampling current k and to detect whether a short-circuit fault occurred. Once a fault was detected, the current-zero prediction algorithm was set up to calculate the coefficients of the short-circuit current and output the current-zero information.

The feasibility of the fault current-zero prediction program was validated in RTDS (i.e., Real-time Digital Simulation system). The essential time to predict the fault current-zero was verified to be 4.0 ± 0.4 ms for different fault initiation phase-angles, signal-to-noise ratios (SNRs), harmonic components, and basic frequencies. In the validation, the fault-initiated phase-angle ranged from 0° to 360° in steps of 10°. The SNR rose from 10 to 20 and 30 dB. The harmonic components included the fifth and seventh harmonics with amplitudes that were 10% of the basic frequency of the fault current. The basic frequency ranged from 49.5 Hz to 50.5 Hz in steps of 0.1 Hz.

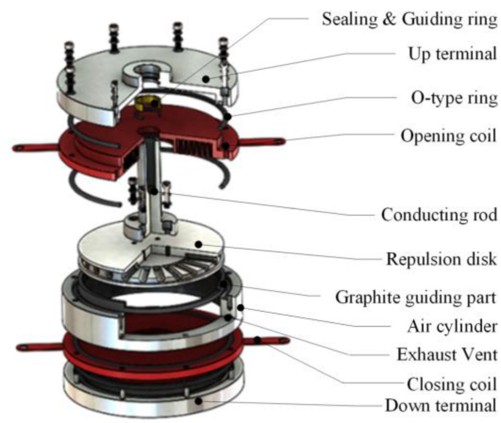

Fig. 4. Exhaustive view of the optimized ERA integrated with the gas damper.

C. Optimization of the ERA with Low Deviations

It was necessary to optimize the ERA with a low deviation of opening time for the CFVB technology to perform an accurate opening operation. The deviations were mainly caused by deformations of the components in the dynamic transmission system, which were due to the high impact force in closing and opening operations of the FVCB. A gas damper was integrated into the ERA to lower the impact force by providing a buffering force in the end-phase of closing and opening operations. The gas damper works based on the differential pressure between the chamber in the moving direction and that in the opposite direction. Both chambers are separated by a repulsion disk. Series of exhaust vents, with a diameter of 1.0 mm, are machined in the air cylinder of the actuator to release the compressed air in the end phase of operations. Fig. 4 shows the exhaustive view of the optimized ERA geometry.

A multi-physics coupled simulation method was adopted to optimize the ERA configuration by considering the multibody dynamics, fluid-solid coupled field, and eddy current electromagnetic field. The optimization aimed to lessen the impact force of the ERA at high closing and opening speed. Table I shows the parameters of the optimized ERA. The optimized moving mass of dynamic transmission system of the FVCB decreased from the original 7.5 kg to 4.5 kg. The optimized closing and opening speed of the FVCB was 2.5 m/s and 5.2 m/s, respectively. The speed was defined as average speed in the first half contact stroke of 20 mm in the moving direction. The closing and opening times and their deviations were found to be 12.5 ± 0.3 ms and 2.5 ± 0.05 ms, respectively, after 2000 opening and closing operations.

TABLE I
PARAMETERS OF THE OPTIMIZED ERA

Items	Symbol	Units	Quantity
Turns of opening & closing coils	N	——	15
Hight of opening & closing coils	H	mm	15
Inner diameter of opening & closing coils	r	mm	60
Outer diameter of opening & closing coils	R	mm	200
Thickness of repulsion disk	T	mm	15
Diameter of repulsion disk	D	mm	200
Air gap between disk and coils	δ	mm	1.0
Opening & Closing capacitors	C	mF	15
Charged voltage of opening capacitor	U_{op}	kV	0.65
Charged voltage of closing capacitor	U_{clo}	kV	0.65
Moving mass of the 40.5 kV FVCB	m	kg	4.5

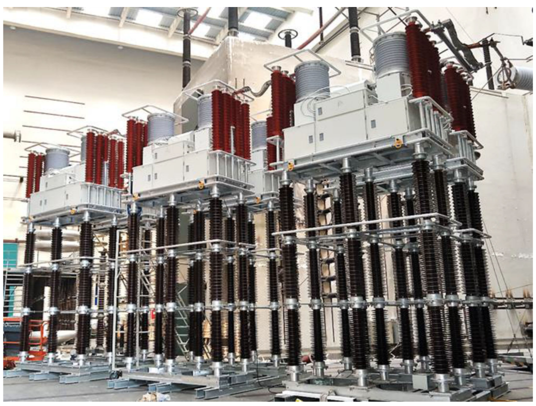

Fig. 5. Photograph of a single-phase 363 kV/5000A-63 kA FVCB under testing.

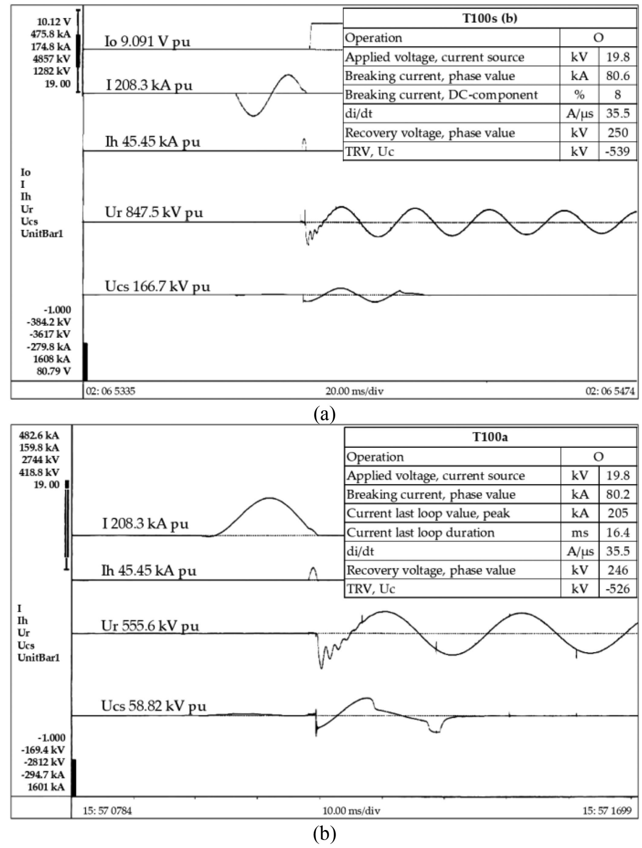

Fig. 6. Test records of the terminal fault test duties: (a) symmetrical short-circuit current interruption test duty T100s(b) and (b) asymmetrical short-circuit current interruption test duty T100a.

III. VALIDATION OF THE CFVB TECHNOLOGY

A single-phase prototype of multiple-break 363 kV FVCB was used to confirm the feasibility of the CFVB technology. The rated current of the prototype is 5000 A, and the rated short-circuit breaking current is 63 kA. Fig. 5 shows the photograph of the prototype under testing. The prototype consists of two parallel-connected circuit branches, with each branch comprising six series-connected 40.5 kV FVCBs. The opening time of the prototype, from triggering of opening operation to contacts separation of the last break, is 2.5 ms. The opening speed in the first half contact stroke of 20 mm for each 40.5 kV FVCB is 5.2 m/s. A short-arcing time of 2.5 ms is assigned to the porotype in a purpose that it can eliminate the short-circuit fault in the first half-wave fault current.

The test duties of symmetrical short-circuit breaking test T100s(b) and asymmetrical short-circuit breaking test T100a were both conducted following the requirement of international standard IEC 62271-100 and Chinese standard GB/T 1984–2014. Fig. 6 shows typical test records of T100s(b) and T100a with a prospective breaking current of 80 kA rms. The test results demonstrated the prototype could handle a current interruption of 80 kA rms within the first half-wave fault current with a short-arcing time of 2.5 ms.

Further application of the controlled fast vacuum breaking technology could benefit power distribution and transmission systems from more reliable operations, high power energy transmission capacities, low costs of RAMS (i. e. reliability, availability, maintainability, and safety), and enhanced accessing of new clean energy. Also, in achieving high operating reliability of resistive-type high-temperature superconductivity (HTS) based SFCL, the CFVB technology could be adopted to effectively moderate the thermal stress imposed and accumulated in the HTS tapes.

IV. CONCLUSION

This paper proposed CFVB technology for an AC short-circuit fault elimination within a short-arcing time. The technology operates in the following sequence: 1) determining a lower-limit opening speed for the FVCB to perform a reliable high current interruption, 2) quickly predicting the fault current-zero to command the FVCB to open at a selected current phase-angle, and 3) optimizing the ERA integrated with a gas damper for a low deviation of low opening time to achieve an accurate opening operation. The CFVB technology was deployed in a single-phase 363 kV multiple-break FVCB to validate its feasibility by performing test duties of T100s(b) and T100a following standards IEC 62271-100 and GB/T 1984–2014. Test results proved that the CFVB technology can eliminate a short-circuit fault within the first half-wave fault current. Further application of the CFVB technology would contribute to promoting the transient stability of the power grid.

REFERENCES

[1] B. S. Karasik, I. I. Milostnaya, M. A. Zorin, A. I. Elantev, G. N. Gol'tsman, and E. M. Gershenzon, "High speed current switching of homogeneous YBaCuO film between superconducting and resistive states," *IEEE Trans. Appl. Supercond.*, vol. 5, no. 2, pp. 3042–3045, Jun. 1995.

[2] Y. J. Tang, T. Kato, N. Hayakawa, Y. Yokomizu, T. Matsumura, H. Okubo *et al.*, "Development of the prospective power transmission model system integrated under superconducting environment-PROMISE," *IEEE Trans. Appl. Supercond.*, vol. 5, no. 2, pp. 945–948, Jun. 1995.

[3] Working Group 10, "Fault current limiters in electrical medium and high voltage systems," Technic Brochure 239, CIGRE Study Committee SC A3 (High Voltage Equipment), Dec. 2003.

[4] H. Kojima, T. Osawa, and N. Hayakawa, "Fault current limitation coordination in power transmission system with superconducting fault current limiting cables (SFCLC)," *IEEE Trans. Appl. Supercond.*, vol. 25, no. 3, Jun. 2015, Art. no. 5401904.

[5] M. Ichikawa and M. Okazaki, "A magnetic shielding type superconducting fault current limiter using a Bi2212 thick film cylinder," *IEEE Trans. Appl. Supercond.*, vol. 5, no. 2, pp. 1067–1070, Jun. 1995.

[6] Y. Tan *et al.*, "Repulsion mechanism applied in resistive-type superconducting fault current limiter," *IEEE Trans. Appl. Supercond.,* vol. 26, no. 6, Sep. 2016, Art. no. 5602009.

[7] R. Smeets, L. Sluis, M. Kapetanovi, D. F. Peelo, and A. Janssen, *Switching in Electrical Transmission and Distribution Systems*, 1 ed. West Sussex, U.K.: Wiley Ltd, 2015, pp. 243–258.

[8] I. Hiroki, *CIGRE Green Book: Switching Equipment*. Cham, Switzerland: Springer, 2019, pp. 157–294.

[9] W. Jinn-Chang, J. Hurng-Liahng, W. Kuen-Der, and S. Nan-Tsun, "Hybrid switch to suppress the inrush current of AC power capacitor," *IEEE Trans. Power Deliv.*, vol. 20, no. 1, pp. 506–511, Jan. 2005.

[10] Z. Bojian *et al.*, "A relationship between minimum arcing interrupting capability and opening velocity of vacuum interrupters in short-circuit current interruption," *IEEE Trans. Power Deliv.*, vol. 33, no. 6, pp. 2822–2828, Dec. 2018.

[11] J. Maguire *et al.*, "Development and demonstration of a fault current limiting HTS cable to be installed in the con edison grid," *IEEE Trans. Appl. Supercond.*, vol. 19, no. 3, pp. 1740–1743, Jun. 2009.

[12] X. Yao, C. Guan, J. Wang, Y. Geng, Z. Liu, and X. Zhai, "Optimizing the opening velocity for a vacuum circuit breaker with cup-type axial magnetic field contacts," *IEEE Trans. Plasma Sci.*, vol. 49, no. 5, pp. 1636–1647, May 2021.